Results S1: screening for mutations in known RP genes

Selection of non-synonymous variants in RP genes yielded an average of 84 variants (*vars*) per genome (Figure S1). For the sake of clarity, we define the term *var* to indicate a unique variation in the genome regardless of its number of copies. Therefore, both a homozygous and a heterozygous DNA variant at a given genomic position and of a given type (e.g. G>A) were considered as a single *var*. When variants reported in the dbSNP at a frequency ≥ 2% were removed from the filtered list, an average of 8 *vars* remained per genome. Imposing the presence of 2 variants (mutant alelles) per gene, typical of the inheritance of a recessive trait, yielded only 1 *var* on average (range: 0 to 4) per genome. All of these changes were retrospectively cross-checked again with dbSNP 131, and none of them was present in the database. No significant difference in the efficiency of the filtering process was found between North American and Japanese genomes (Supplementary Table S3).

In parallel to this process, we also analyzed the information deriving from discordant mate pair sequences, in order to detect less frequent and larger structural variations, typically sized over a few hundred bases. Specifically, we highlighted all sequences originating from mate pairs that carried inconsistencies in terms of distance and/or orientation with respect to the reference sequences. Reliable mate pair information appeared to be heavily dependent on the quality of the template DNA that was sequenced. In our study, only 7 genomes (003-019, 003-050, 218-304, 219-004, R4, R8, and R9), corresponding mostly to samples that were recently isolated, produced consistent output. Accordingly, samples that did not provide consistent mate-pair mapping information were predominantly older DNAs, some collected over a

decade ago. Re-sequencing of two of these samples yielded the same results, reinforcing the notion that DNA age, rather than the sequencing procedure *per se*, was the cause of this specific problem. In the seven genomes with reliable mate-pair mapping, we found 2 SVs each affecting the coding sequence of an ARRP gene in two different genomes (*USH2A* in patient 003-019 and *EYS* in patient R9, Figure 2). Both individuals had another novel non-synonymous variant in the same gene detected through the mapping of short reads, accounting for the autosomal recessive pattern of inheritance.

Next, the list of candidate mutations was further narrowed by performing a literature search, to exclude variants that had been reported previously as non-pathogenic in publications, but not in dbSNP 131. The resulting list of candidate gene-variations is summarized in Table S2. No candidate gene-variations were present in 6 genomes. Out of the 16 pathogenic alleles identified, 14 were judged clearly deleterious, comprising 6 nonsense mutations, 4 frameshift mutations, 2 splice site mutations, and the 2 SVs mentioned above. Two missense mutations, p.G76R in *RDH12* and p.C3294W in *USH2A*, were also considered pathogenic. p.G76R has been associated with RP previously (1) and was identified together with another nonsense mutation (p.R84X) in the same gene. p.C3294W in *USH2A* was identified together with the 2,229 bp deletion, causing the inframe ablation of Exon 27. C3924 is located in the functionally poorly-characterized stretch of residues flanked by two Fibronectin III domains in which 13 CC repeats are present. This dicysteine-rich domain was previously recognized by Baux *et al.* (2) and found to harbor 4 disease causing mutations affecting such repeats (2-4) (Figure 2). p.C3294W disrupts the 8th cysteine pair of this conserved CC repeat structure. Taken together, the evidence highlighted

the importance of C3294 and indicated the pathogenicity of the p.C3294W mutation. It is also of note that novel homozygous pathogenic mutations were identified in *PDE6B* and *DFNB31* in Japanese patients with parental history of consanguinity. These mutations were both located inside the long genomic stretches of high homozygosity predicted to be IBD.

In 6 out of the 8 patients with pathogenic alleles in a known RP gene, no other candidate genes were present after the series of filtering process, yielding unambiguous genetic diagnosis. Meanwhile, the remaining two patients carried 1 or 2 additional candidate genes, i.e. genes carrying 2 rare variants. However, all of these variants were missense changes affecting poorly conserved residues. They were excluded as candidate mutations, given the presence of 2 clear pathogenic alleles and are not displayed in Table S2.

In addition to the 8 patients in whom 2 clearly pathogenic alleles were identified and whose genetic etiology can be considered as solved, two patients had at least one pair of variant alleles in a known ARRP gene that could potentially account for the disease. In R15, a homozygous missense change (p.V164F) was found in *USH2A* in the presumed IBD region. However, we found another homozygote for the same change in one of the 95 ethnically matched controls, thus we considered this variant to be non-pathogenic. In the same patient, we found a pair of missense variants (p.E604K and p.F1118L) in a compound heterozygous state in the *RPGRIP1L* gene. p.E604K was found in dbSNP build 134 (rs143863631); however, its allelic frequency was less than $5x10^{-4}$ and was therefore compatible with that of a rare mutation. p.F1118L was found in an exon belonging to an alternative splicing isoform of

RPGRIP1L. A database search (tblastn) revealed this exon to be present in primates only, at least based on the currently-available genomic information. We therefore considered *RPGRIP1L* as a possible, although unlikely, candidate gene for ARRP in this individual. Another Japanese patient, R19, carried two homozygous missense changes in *USH2A* (p.I3620T and p.P3114S) in the putative IBD region. p.P3114S is unlikely to be pathogenic because a serine residue at codon 3114 is found in various mammals and lower vertebrates. Meanwhile p.I3620, located in the Fibronectin III domain, is conserved not only among most *USH2A* homologues ranging from non-vertebrates to primates but also among the amino acids defining the domain itself. Although codon 3620 is not invariant in humans (the minor allele of SNP rs145207584 leads to a p.I3620V change in ~0.8% of the control population), p.I3620T was not found among 477 Japanese controls. However, as we lacked the critical information to link p.I3620T to the disease development, we classified the variant as of uncertain significance. In the same patient, another pair of heterozygous novel missense changes was identified in *SPATA7* (p.D265V, c.794A>T and p.M313V, c.937A>G). p.M313V was considered non-pathogenic because p.V313 was found in various mammals and in dbSNP. Therefore, this variant and thus *SPATA7* was considered unrelated to the disease in this patient.

We found additional clearly deleterious mutations in three genes in three patients. They were not considered to be responsible for ARRP in these individuals and were not reported in Table S2 since they were all found in a heterozygous state, with no second mutation in the same gene. More specifically, a frameshift mutation in *DFNB31* (p.K213fs) was identified in R14. This was however considered not to be causative of the disease since R14 is also a carrier of a homozygous pathogenic

PDE6B splice site mutation. Frameshift mutations in *SPATA7* (p.V7fs, c.20_3delTCAG) and *EYS* (p.S1653fs, c.4957_4958insA) were identified in R8 and R16, respectively. The etiology of both patients remained unsolved at this point as no additional candidate variants in the exons of these genes to account for ARRP were identified. More intensive search targeting all conserved elements in non-exonic regions of genes, including promoter and introns, in these two genomes revealed no additional candidate pathogenic variants.

References

1. Aldahmesh MA, et al. (2009) Molecular characterization of retinitis pigmentosa in Saudi Arabia. *Mol. Vis.* 15:2464-2469.
2. Baux D, et al. (2007) Molecular and in silico analyses of the full-length isoform of usherin identify new pathogenic alleles in Usher type II patients. *Hum. Mutat.* 28:781-789.
3. McGee TL, Seyedahmadi BJ, Sweeney MO, Dryja TP, Berson EL (2010) Novel mutations in the long isoform of the USH2A gene in patients with Usher syndrome type II or non-syndromic retinitis pigmentosa. *J. Med. Genet.* 47:499-506.
4. Aller E, et al. (2006) Identification of 14 novel mutations in the long isoform of USH2A in Spanish patients with Usher syndrome type II. *J. Med. Genet.* 43:e55.

Results S2: screening for mutations in all annotated human protein-coding genes

From the total of 3.8 million *vars* included on average in each genome, only non-synonymous variations were initially selected, which yielded an average of 10,881 *vars*. Further filtering out of the variants by cross-comparison with dbSNP resulted in 1,108 *vars*, which were reduced again to 508 after excluding those that were present in the 69 publicly available control genomes. When only variants found in either homozygous or compound heterozygous state were selected, 59 *vars* for a total of 29 genes per genome remained in the list. All these variants could potentially cause ARRP and thus were regarded as potential candidate mutations.

At this point, our strategy was supplemented with a process of phenotype-genotype association for the few promising genes/mutations surviving the previous filtering processes. Annotation of all the candidate genes through *in silico* analysis of their association with known retinal function or phenotype, tissue expression, and potential regulation by the photoreceptor-specific transcription factor CRX revealed no candidate gene with an outstanding profile. Therefore, we further prioritized DNA variants based on the severity of the variation produced, by retaining genes that had at least 1 clearly deleterious change (nonsense, nonstop, misstart, frameshift, or invariant splice site change). After this process, we were left with an average of 5 *vars* in 4 genes per genome. Application of this stringent filtering criterion to the 8 genomes with definite ARRP molecular etiology still ensured that all of the pathogenic mutations identified in the known RP genes were included. Notably, we did not observe any overall difference in the efficiency of the filtering process between Japanese and

American patients except for the number of homozygous candidate variations, for which enrichment was observed in Japanese patients with parental consanguinity (Supplementary Table S4).

In parallel, we also devised an analytical pipeline for SVs with mate-pair mapping (Supplementary Figure S3). Among an average of 4,122 SV *vars* derived from 7 genomes with reliable mappings, 933 were not found in 52 normal controls. Further selection of SVs affecting mRNA resulted in 211 *vars*, 37 of which were supported by 10 or more mate pairs and were considered to be reliable. When SVs affecting the coding sequence were selected, only 6 *vars* remained as potential pathogenic candidates per genome, on average. However, none of these SVs were in a compound heterozygous state with other SVs or with candidate variations detected through mapping of the short reads in the unsolved genomes, thus they were not considered to be candidate variants.

Next, literature search was conducted on the pairs of candidate gene-variations for which at least one of the alleles was clearly deleterious. This process aimed at excluding genes with known association with non-ocular Mendelian diseases and to remove reported non-pathogenic variants not enrolled in dbSNP. Genes for which lack of functional relevance could be inferred, based on the lack of retinal phenotype in the mice defective of the homologous genes, were also excluded. As a result of this process, only 2 candidate genes in 2 genomes remained among the 8 unsolved cases. No candidate was found in the remaining 6 genomes after this annotation process. In R15, we found a homozygous frameshift mutation (p.R165fs, c.494delG) in the *ITIH5* gene in an IBD region. However, this variant was considered

non-pathogenic because another homozygous frameshift mutation (p.D719fs; rs71806144) in *ITIH5* was found in multiple publicly available control genomes.

Supplementary Table S1. General information on the WGS output. Unless stated otherwise, numbers refer to "*vars*", defined as unique variations within the genome, regardless of their allelic information, so that both homozygous and heterozygous variants are considered a single *var*.

	Americans average	**Japanese average**	**Total average**
Gross mapping yield (Gb)	199.4	202.3	200.8
Average coverage (per base)	65.5	66.8	66.1
Fraction of genome covered more than 30x	0.89	0.86	0.875
Called genomic fraction	0.970	0.966	0.968
Total variations	3,972,326	3,758,035	3,865,180
Total novel variations	329,608	272,551	301,079
Total novel rate	0.0814	0.0725	0.0769
Variations not in mRNA	3,950,758	3,737,505	3,844,131
Variations in mRNA	21,569	20,530	21,049
Synonymous	10,499	9,948	10,224
Non-synonymous	11,069	10,582	10,826
Missense	10,068 (91.0%)	9,549 (90.2%)	9,808 (90.6%)
Nonsense	97 (0.9%)	96 (0.1%)	96 (0.9%)
Nonstop	18 (0.2%)	12 (0.1%)	15 (0.1%)
Misstart	19 (0.2%)	29 (0.3%)	24 (0.2%)
Frameshift	278 (2.5%)	272 (2.6%)	275 (2.5%)
Frame-preserving	538 (4.9%)	532 (5.0%)	535 (4.9%)
Splice site	52 (0.5%)	92 (0.9%)	72 (0.7%)

Supplementary Table S2. Summary of variants found in known ARRP genes in the 16 index cases. Abbreviations; F, female; M, male; N, no; Y, yes; Cons., reported parental consanguinity; hom, homozygous; het, heterozygous.

Patient ID	Sex	Cons.	Ethnicity	Gene	Protein change	DNA change	State	Interpretation
003-019	F	N	Mixed European	*USH2A*	p.C3294W	c.9882C>G	het	pathogenic
				USH2A		del Ex27	het	pathogenic
003-050	M	N	Mixed European					no candidates
003-175	F	N	Mixed European					no candidates
003-197	F	N	Haitian	*RDH12*	p.R84X	c.250C>T	het	pathogenic
				RDH12	p.G76R	c.226G>T	het	pathogenic
099-046	F	N	Hispanic	*CNGB1*	p.C632X	c.1896C>A	het	pathogenic
				CNGB1	p.G1050fs	c.3150delG	het	pathogenic
218-304	M	N	Mixed European	*CERKL*	p.T260fs	c.780delT	het	pathogenic
				CERKL	p.K200X	c.598A>T	het	pathogenic
219-004	M	N	Mixed European	*CERKL*	p.R257X	c.769C>T	het	pathogenic
				CERKL	p.L140fs	c.420delT	het	pathogenic
218-237	F	N	Mixed European					no candidates
R4	F	N	Japanese					no candidates
R8	M	N	Japanese					no candidates
R9	F	N	Japanese	*EYS*	p.L1723fs	c.5168_5169insT	het	pathogenic
				EYS	unknown	invert-dup Ex23-29	het	pathogenic

R14	F	Y	Japanese	*PDE6B*	unknown	IVS11+1G>C	hom	pathogenic
R15	F	Y	Japanese	*USH2A*	p.V164F	c.490G>T	hom	non-pathogenic
				RPGRIP1L	p.E604K	c.1810G>A	het	uncertain
				RPGRIP1L	p.F1118L	c.3352T>C	het	non-pathogenic
R16	F	Y	Japanese					no candidates
R18	F	Y	Japanese	*DFNB31*	p.Q54X	c.160C>T	hom	pathogenic
R19	F	Y	Japanese	*USH2A*	p.I3620T	c.10859T>C	hom	uncertain
				USH2A	p.P3114S	c.9340C>T	hom	non-pathogenic
				SPATA7	p.D297V	c.1041A>T	het	uncertain
				SPATA7	p.M345V	c.1183A>G	het	non-pathogenic

Supplementary Table S3. Analysis of known ARRP genes. Numbers refer to "*vars*", unless stated otherwise. T-test was computed from absolute values from American vs. Japanese patients.

	Total ave	**Americans ave**	**Japanese ave**	**T-test**
Non-synonymous in RP genes	84	88	80	0.015
Novel or frequency < 2%	8	9	8	0.413
Frequency >= 2%	76	79	72	0.060
Two or more alleles per gene	1	1	1	0.549
One allele per gene	7	8	7	0.457

Supplementary Table S4. Analysis of all known genes. Numbers refer to mean values of "*vars*", unless stated otherwise. T-test was computed from absolute values from American vs. Japanese patients. "cons.", consanguineous.

	All patients	Americans	Japanese Total	Japanese Cons.	Japanese Non-cons.	T-test
Non-synonymous	10881	11108	10655	10905	10239	0.26
Novel	1108	1124	1093	1114	1057	0.76
In dbSNP	9773	9984	9562	9791	9182	0.18
Not in 69 controls	508	485	531	550	501	0.46
In controls	600	639	562	564	556	0.08
Two or more alleles per gene						
Total vars	59	54	64	75	45	0.60
Total genes	29	25	33	40	23	0.35
Homozygous	9	4	14	19	5	0.01
Homoz. in IBD (cons. only)				14		
One allele per gene	449	431	468	475	455	0.42
>= 1 deleterious variant per gene						
vars	5	5	5	7	1	0.95
genes	4	4	4	7	1	0.82
Others	54	49	59	67	45	0.58

Supplementary Table S5. List of 64 genes used for the selective analysis of ARRP-associated genes.

ABCA4
AGTPBP1
AIPL1
C2orf71
CABP4
CDH23
CEP290
CERKL
CLN8
CLRN1
CNGA1
CNGB1
CRB1
CRX
CYP4V2
DFNB31
DHDDS
EYS
FAM161A
GPR98
GRK1
GUCY2D
IDH3B
IMPG2
IQCB1
KCNJ13
KCNV2
LCA5
LRAT
MAK
MERTK
MYO7A
NR2E3
NRL
PCDH15
PCDH21
PDE6A
PDE6B
PDE6G
PHYH
PRCD
RBP3
RBP4
RD3
RDH12
RGR
RHO
RLBP1
ROM1
RP1
RP2
RPE65
RPGR
RPGRIP1
RPGRIP1L
SEMA4A
SPATA7
TTC8
TTPA
TULP1
USH1C
USH1G
USH2A
ZNF51

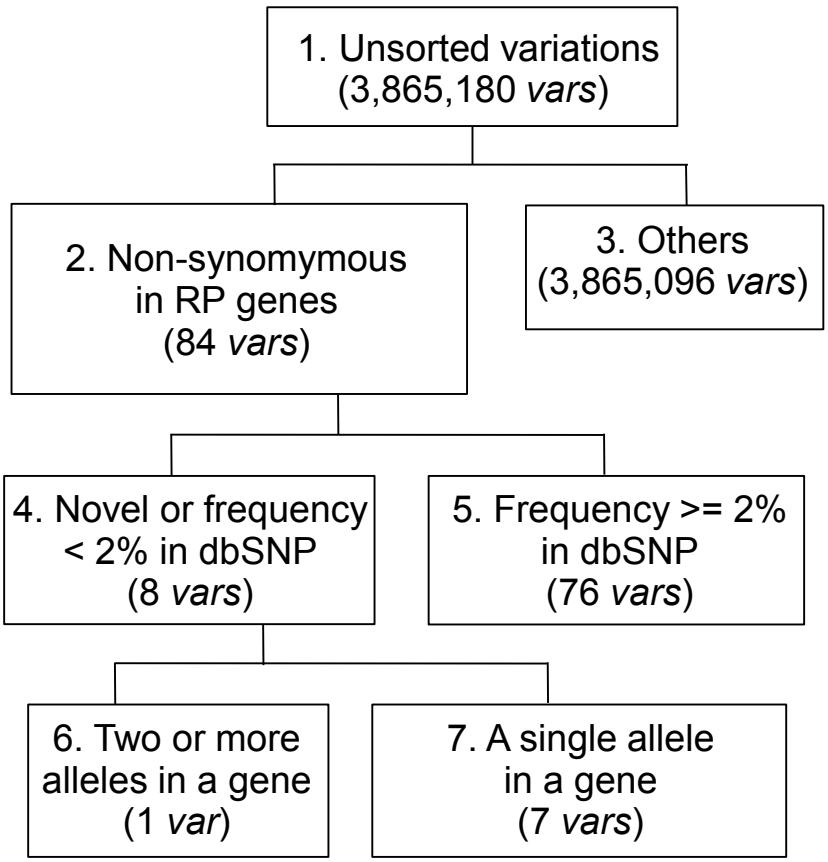

Supplementary Figure S1. Flow chart of the filtering process for variants in known ARRP genes. Numbers represent average values over all 16 genomes.

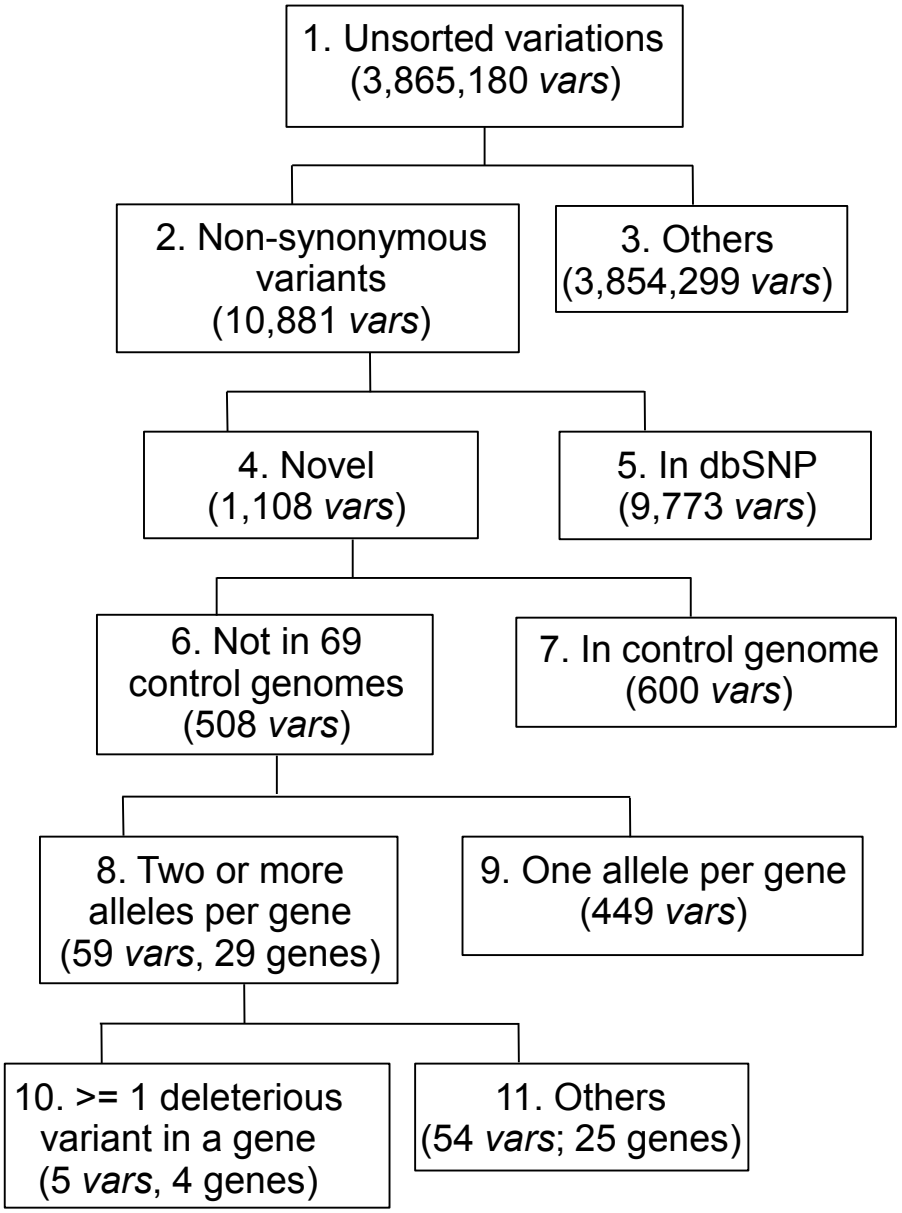

Supplementary Figure S2. Flow chart of the filtering process for the systematic variant detection in all genes. Numbers represent average values over all 16 genomes.

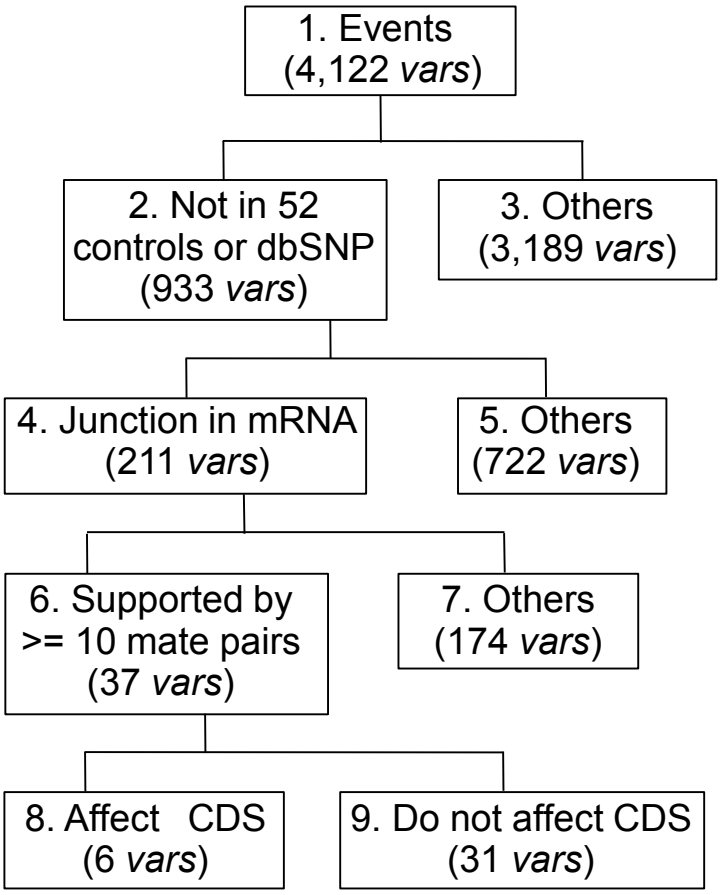

Supplementary Figure S3. Flow chart of the filtering process for structural variations.

Numbers represent average values over all 7 genomes with reliable output.

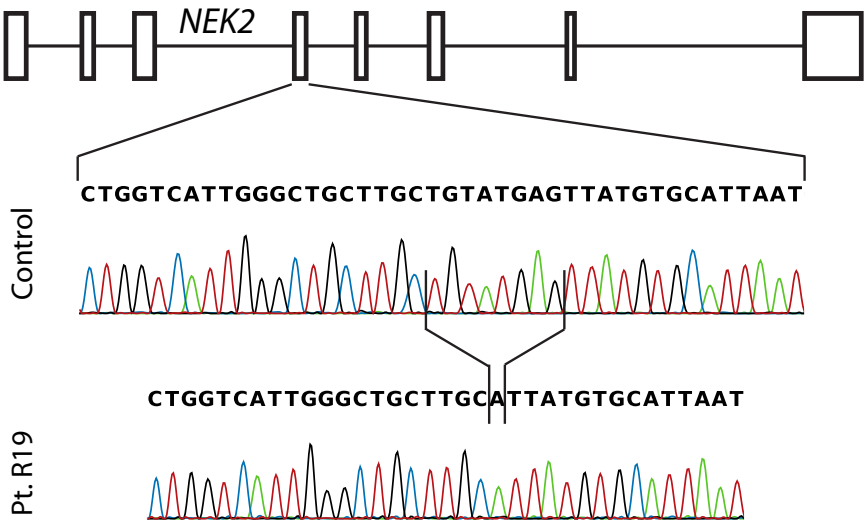

Supplementary Figure S4. The homozygous mutation p.L206fs identified in patient R19. The schematic structure of the gene *NEK2* is provided; exons are indicated by boxes, introns by solid lines. Chromatograms document the concurrent deletion of 8 bases and the insertion of an additional adenosine in the patient, compared to a control sequence.

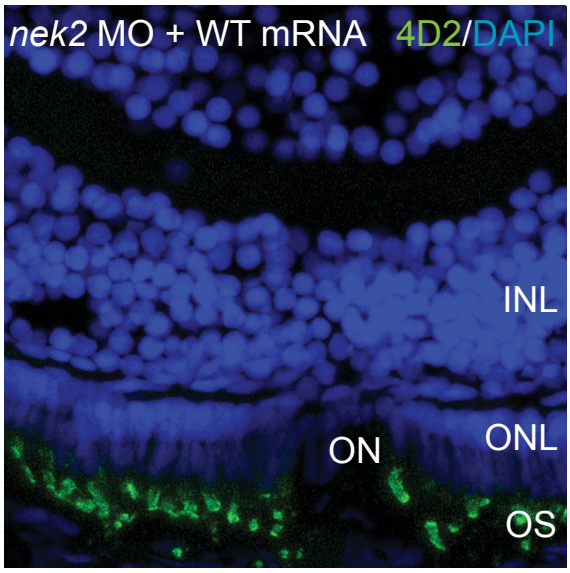

Supplementary Figure S5. *In vivo* rescue of *nek2* deficiency in zebrafish by human *NEK2* mRNA supplementation. Immunohistochemical analyses of retinal cryosections from *nek2* MO embryos + human wt *NEK2* mRNA, stained with DAPI (blue) and 4D2 antibody (green). INL, inner nuclear layer; ONL, outer nuclear layer; ON, optic nerve; OS, outer segment of photoreceptors.

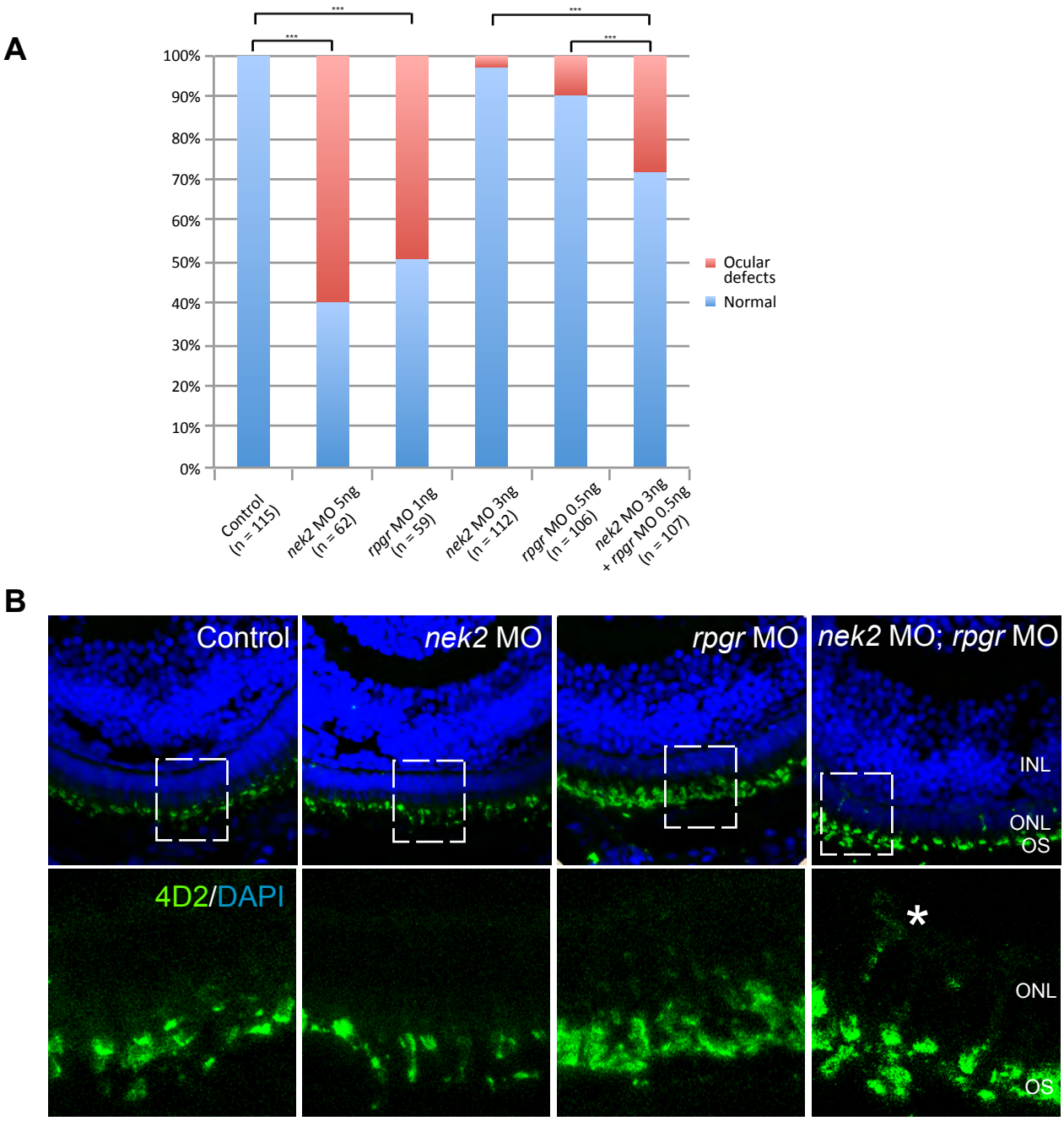

Supplementary Figure S6. *In vivo* functional evaluation of *nek2* and *rpgr* deficiency in zebrafish. (**A**) Ocular phenotypes are quantified in control, *nek2* MO, *rpgr* MO, and *nek2* MO + *rpgr* MO embryos at full and sub-effective doses. (**B**) Immunohistochemical analyses of retinal cryosections from control, *nek2* MO, *rpgr* MO, and *nek2* + *rpgr* MO embryos at sub-effective doses, stained with DAPI (blue) and 4D2 antibody (green). Asterisk denotes excessive rhodopsin in the outer nuclear layer (ONL). OS, outer segment of photoreceptors; INL, inner nuclear layer.

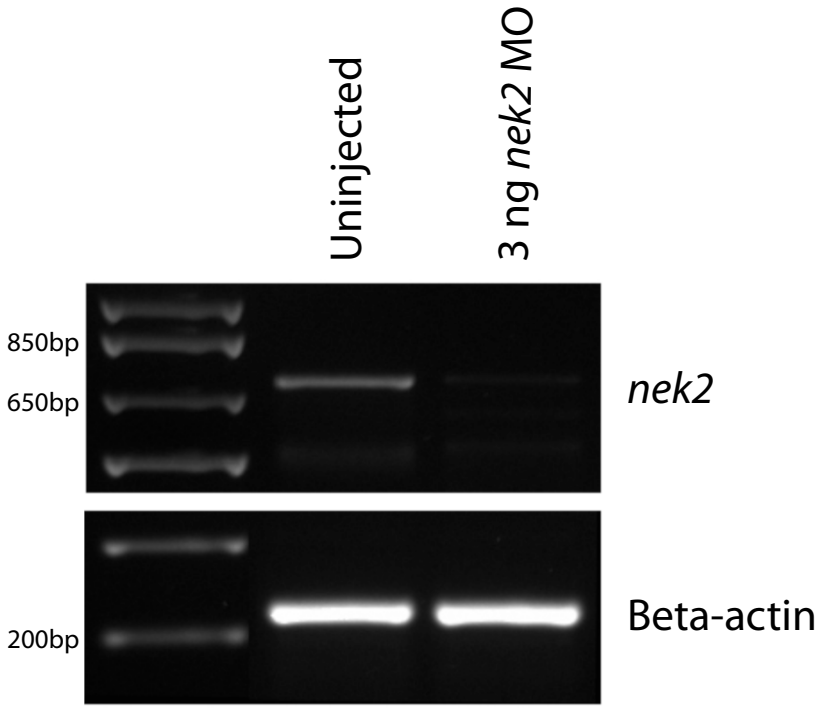

Supplementary Figure S7. Effects of MO against *nek2* in zebrafish on the targeted gene. Beta-actin represents a negative control.

Methods

Patients and controls

Leukocyte DNA was obtained for WGS from 8 patients from the Berman-Gund Laboratory, Harvard Medical School, Massachusetts Eye and Ear Infirmary. These patients had a family history indicative of an autosomal-recessive form of inheritance; no ARRP mutations were previously identified. Six patients were of mixed European ancestries (003-019, 003-050, 003-175, 218-237, 218-304, and 219-004), 1 was of Haitian ancestry (003-197), and 1 was a Hispanic from Puerto Rico (099-046). Leukocyte DNA was also prepared for WGS from 8 patients (R4, R8, R9, R14, R15, R16, R18, and R19) of Japanese ancestry from the Nagoya University Hospital. They had RP with no family history (isolate RP) or a family history indicative of ARRP. Five of them (R14, R15, R16, R18, and R19) reported parental consanguinity.

All 16 patients analyzed with WGS (3 males and 13 females) had typical RP documented by comprehensive clinical testing including ERG, visual field testing, and fundus examination and were judged to have a non-syndromic form of the disease based on the lack of significant non-ocular medical history and symptoms. Comprehensive genomic data from patients were not made publicly available since this option was not included in the consent forms.

Genomes from 69 healthy individuals, sequenced according to the same methodology and publicly available at ftp://ftp2.completegenomics.com, were used as controls for variations obtained from the mapping of short reads within patients' genomes. For the analysis of structural variants (SVs) and non-coding RNA, 52 out of 69 genomes, representing unrelated individuals within this set, were used for controls.

Moreover, some variations were further screened in a cohort of 95 healthy North Americans, 95 healthy Japanese, or both by Sanger sequencing. Other 1,178 Japanese control individuals (2,356 chromosomes) were screened for the presence of the *NEK2* p.L206fs mutation by next-generation sequencing, targeted PCR, or both.

Additional DNA samples from 13 patients (10 families) with ARRP or other recessive retinal degenerations and showing linkage to the chromosomal region containing *NEK2* were provided by members of the European Retinal Disease Consortium and were screened for mutations in the coding parts of *NEK2* by Sanger sequencing.

Whole genome sequencing (WGS)

WGS was performed by Complete Genomics Inc. (Mountain View, CA, USA) as described previously (1). The reference sequence used for the mapping was the one provided by NCBI in build 37 of the human genome. The variations were further annotated with respect to their presence or absence in the dbSNP database build 131.

Analysis of the mapping results

In silico analyses were performed by programs and scripts developed in-house, as well as by the use of the “CGA tools” provided by Complete Genomics (http://www.completegenomics.com/sequence-data/cgatools/). Non-synonymous variants were classified as missense, nonsense, nonstop (nucleotide change in the stop codon resulting in the abnormal continuation of the coding sequence), misstart (non-synonymous change in the start codon, likely resulting in non-functional gene), frameshift, frame-preserving (inframe deletions, insertions, or substitutions), and splice

site (variations affecting the +1, +2, -1, and -2 invariant bases of the splice donor or acceptor sites).

A total of 64 genes reported to be associated with ARRP and allied diseases including LCA and cone-rod dystrophy, a form of retinal degeneration characterized by initial predominant loss of cone function with some reduction of rod function (2), were selected for the targeted analysis of known disease-associated genes (Supplementary Table S5). Genes usually associated with syndromic ARRP were selected only if they were also involved in the non-syndromic form of this disease. In addition, all genes linked to Usher syndrome were included in the list because of the relatively high frequency of their association with non-syndromic ARRP (3, 4). The reference sequence (mRNA, protein) used for the annotation of *USH2A*, *RDH12*, *CNGB1*, *EYS*, *PDE6B*, *DFNB31*, *CERKL*, *RPGRIP1L*, *SPATA7*, *ITIH5*, and *NEK2* were (NM_206933.2, NP_996816.2), (NM_152443.2, NP_689656.2), (NM_001297.4, NP_001288.3), (NM_001142800.1, NP_001136272.1), (NM_000283.3, NP_000274.2), (NM_001083885.2, NP_001077354.2), (NM_201548.4, NP_963842.1), (NM_015272.2, NP_056087.2), (NM_018418.4, NP_060888.2), (NM_030569.4, NP_085046.4) and (NM_002497.3, NP_002488.1), respectively. Nucleotide references for all DNA variants described reflect cDNA numbering with +1 corresponding to the A of the ATG translational initiation codon.

All the candidate genes that were not known to be linked to ARRP were assessed for their association with other retinal phenotypes (Online Mendelian Inheritance in Man; http://www.ncbi.nlm.nih.gov/omim), their mRNA expression in the eye (UniGene; http://www.ncbi.nlm.nih.gov/UniGene), or the binding of the

photoreceptor-specific transcription factor cone-rod homeobox (CRX) to the promoter and intronic region of mouse homologues, via ChIP-seq (5). All variants for which pathogenicity was suspected underwent verification via PCR and Sanger sequencing, according to standard protocols.

Determination of homozygosity by HomozygosityMapper

Determination of genomic regions of high homozygosity likely derived from the same ancestral allele (i.e. identical by decent; IBD) was conducted using the web-based tool HomozygosityMapper (http://www.homozygositymapper.org/) (6). In brief, the genotypes of the 592,652 SNPs listed in the Illumina 660W array (Illumina Inc., San Diego, CA, USA) were extracted from the sequenced genomes and used as an input to the program, which calculated and displayed the genomic area with high homozygosity, likely to be IBD.

Zebrafish models

Morpholino oligos (MO) against *nek2* and *rpgr* (5'-CAAGATAAAGAACACTTACTGGCGA -3' and 5'-CTTCTGTTTCTCCAGCCATCTCTGC -3' (7), respectively, Gene Tools, Philomath, OR, USA) were designed and validated to silence expression of the endogenous gene (Supplementary Figure S7). Zebrafish embryos at 2- to 8-cell stage were microinjected with 3-6 ng *nek2* MO, and/or 50 pg human NEK2 wild-type mRNA, as previously described (8).

Zebrafish embryos were then grown in embryo medium with 0.003% PTU to prevent pigmentation. At 2 dpf, 3 dpf, 4 dpf, and 5 dpf, embryos were anesthetized in

embryo medium containing 0.2 mg/ml tricaine (Ethyl 3-aminobenzoate methanesulfonate, Sigma, St. Louis, MO, USA), and then fixed with 4% PFA in 1x PBS. The TUNEL assay was carried out with ApopTag Red In Situ Apoptosis Detection Kit (Millipore, Billerica, MA, USA). Fixed embryos were embedded in formalin or PFA, sectioned at 10 µm and stained using Toluidine blue or for an antibody against rhodopsin (4D2, Millipore). Images were captured using a Zeiss 710 confocal microscope, as well as Nikon AZ100 and T90I microscopes, and analyzed/processed using Nikon elements and Adobe Photoshop.

References

1. Drmanac R, et al. (2010) Human genome sequencing using unchained base reads on self-assembling DNA nanoarrays. *Science* 327:78-81.
2. Berson EL, Gouras P, Gunkel RD (1968) Progressive cone-rod degeneration. *Arch. Ophthalmol.* 80:68-76.
3. Rivolta C, Sweklo EA, Berson EL, Dryja TP (2000) Missense mutation in the USH2A gene: association with recessive retinitis pigmentosa without hearing loss. *Am. J. Hum. Genet.* 66:1975-1978.
4. Khan MI, et al. (2011) CLRN1 mutations cause nonsyndromic retinitis pigmentosa. *Ophthalmology* 118:1444-1448.
5. Corbo JC, et al. (2010) CRX ChIP-seq reveals the cis-regulatory architecture of mouse photoreceptors. *Genome Res.* 20:1512-1525.
6. Seelow D, Schuelke M, Hildebrandt F, Nurnberg P (2009) HomozygosityMapper--an interactive approach to homozygosity mapping. *Nucleic Acids Res.* 37:W593-599.
7. Ghosh AK, et al. (2010) Human retinopathy-associated ciliary protein retinitis pigmentosa GTPase regulator mediates cilia-dependent vertebrate development. *Hum. Mol. Genet.* 19:90-98.
8. Stuart GW, McMurray JV, Westerfield M (1988) Replication, integration and stable germ-line transmission of foreign sequences injected into early zebrafish embryos. *Development* 103:403-412.